

Distributed Deep Multilevel Graph Partitioning

Peter Sanders ✉

Karlsruhe Institute of Technology, Germany

Daniel Seemaier ✉

Karlsruhe Institute of Technology, Germany

Abstract

We describe the engineering of the distributed-memory multilevel graph partitioner **dKaMinPar**. It scales to (at least) 8192 cores while achieving partitioning quality comparable to widely used sequential and shared-memory graph partitioners. In comparison, previous distributed graph partitioners scale only in more restricted scenarios and often induce a considerable quality penalty compared to non-distributed partitioners. When partitioning into a large number of blocks, they even produce infeasible solutions that violate the balancing constraint. **dKaMinPar** achieves its robustness by a scalable distributed implementation of the deep-multilevel scheme for graph partitioning. Crucially, this includes new algorithms for balancing during refinement *and* coarsening.

2012 ACM Subject Classification Mathematics of computing → Graph algorithms

Keywords and phrases algorithms, distributed systems, graph partitioning, multilevel algorithm, balancing

Supplementary Material The source code and data has been made available at https://algo2.iti.kit.edu/seemaier/ddeep_mgp/.

Acknowledgements This work was performed on the HoreKa supercomputer funded by the Ministry of Science, Research and the Arts Baden-Württemberg and by the Federal Ministry of Education and Research. This project has received funding from the European Research Council (ERC) under the European Union’s Horizon 2020 research and innovation programme (grant agreement No. 882500).



1 Introduction

Graphs are a central concept of computer science used whenever we need to model relations between objects. Consequently, handling *large* graphs is very important for parallel processing. This often requires to *partition* these graphs into blocks of approximately equal weight with most edges inside the blocks (balanced graph partitioning). Applications include scientific computing, handling social networks, route planning, and graph databases [4].

In principle, *multilevel graph partitioners* (MGP) achieve high quality partitions for a wide range of input graphs G with a good trade-off between quality and partitioning cost. They are based on first iteratively *coarsening* G by contracting edges or small clusters. The resulting small graph G' is then still a good representation of the overall input and an *initial partition* of G' already induces a good partition of G . This is further improved by *uncoarsening* the graph and improving the partition on each level through refinement algorithms.

However, parallelizing multi-level graph partitioning has proved challenging over several decades. While shared-memory graph partitioners have recently matured to achieve high quality and reasonable scalability [2, 11, 12, 16], current distributed-memory partitioners [15, 23, 28] induce a severe quality deterioration and often are not able to consistently achieve feasible (i.e. balanced) partitions. In particular, high quality partitioners do not scale to the number of processing elements (PEs) available in large supercomputers. This situation is exacerbated by the fact that often the number of blocks k should increase linearly in the

number of PEs. Previous systems are not able to directly handle large k running into even larger problems with achieving feasibility.

In this paper, we present **dKaMinPar** which addresses all these issues. Its basis is a distributed-memory adaptation of the deep-multilevel graph partitioning concept [11] that continues the multilevel approach deep into the initial partitioning phase. This makes the large k case much easier and eliminates a parallelization bottleneck due to initial partitioning. Our coarsening and refinement algorithms are based on the label propagation approach previously used in several partitioners [15, 23, 28]. Label propagation [22, 24] greedily moves vertices to other clusters/blocks when this reduces cuts (and does not violate the balance constraint). This is simple, fast, effective and robust even for complex networks. We develop a distributed-memory version with improved scalability, e.g., by using improved sparse-all-to-all primitives. Perhaps the main algorithmic innovation are new scalable distributed techniques allowing to maintain the balance constraint. During coarsening, a maximum cluster weight is approximated by unwinding contractions that lead to overweight clusters. During uncoarsening, block weight constraints are achieved by finding, selecting and applying globally “best” block moves.

The experiments described in Section 6 indicate that our implementation has achieved the main goals. It scales to at least 8192 cores even for complex networks that did not scale on previous distributed solvers. Feasibility is guaranteed, even for large k and quality is typically within a few percent of the shared-memory systems. Section 7 summarizes the results and discusses possible future improvements.

Contributions

- Scalable distributed implementation of deep multilevel graph partitioning.
- Simplicity using label propagation for both contraction and refinement.
- New scalable balanced coarsening and uncoarsening algorithm.
- Extensive evaluation on both large real world networks and huge synthetic networks from 3 input families.
- Quality comparable to shared-memory systems.
- Scalability up to (at least) 2^{13} cores and 2^{39} edges.
- Works both for complex networks and large number of blocks where previous systems often fail.

2 Preliminaries

Notation and Definitions. Let $G = (V, E, c, \omega)$ be an undirected graph with vertex weights $c : V \rightarrow \mathbb{N}_{>0}$, edge weights $\omega : E \rightarrow \mathbb{N}_{>0}$, $n := |V|$, and $m := |E|$. We extend c and ω to sets, i.e., $c(V') := \sum_{v \in V'} c(v)$ and $\omega(E') := \sum_{e \in E'} \omega(e)$. $N(v) := \{u \mid \{u, v\} \in E\}$ denotes the neighbors of v . For some $V' \subseteq V$, $G[V']$ denotes the subgraph of G induced by V' . We are looking for *blocks* of nodes $\Pi := \{V_1, \dots, V_k\}$ that partition V , i.e., $V_1 \cup \dots \cup V_k = V$ and $V_i \cap V_j = \emptyset$ for $i \neq j$. The *balance constraint* demands that for all $i \in \{1, \dots, k\}$, $c(V_i) \leq L_{\max} := \max\{(1 + \varepsilon) \frac{c(V)}{k}, \frac{c(V)}{k} + \max_v c(v)\}$ for some imbalance parameter ε^1 . The objective is to minimize $\text{cut}(\Pi) := \sum_{i < j} \omega(E_{ij})$ (weight of all cut edges), where $E_{ij} := \{\{u, v\} \in E \mid u \in V_i \text{ and } v \in V_j, i \neq j, a$

¹ Traditionally, $L_k := (1 + \varepsilon) \lceil \frac{c(V)}{k} \rceil$ is used as balance constraint. We relax this constraint since it is otherwise NP-complete to find a feasible partition.

boundary vertex. A *clustering* $\mathcal{C} := \{C_1, \dots, C_\ell\}$ is also a partition of V , where the number of blocks ℓ is not given in advance (there is also no balance constraint).

Machine Model and Input Format. The distributed memory model used in this work considers P processing elements (PEs) numbered $1..P$, connected by a full-duplex, single ported communication network. The input graph is given with a (usually balanced) 1D vertex partition. Each PE is given a subgraph of the input graph (i.e., a block of the 1D partition) with consecutive vertices. An undirected edge $\{u, v\}$ is represented by two directed edges (u, v) , (v, u) , which are stored on the PEs owning the respective tail vertices. Vertices adjacent to vertices owned by other PEs are called *interface vertices* and are replicated as *ghost vertices* (i.e., without outgoing edges) on those PEs.

3 Related Work

There has been a huge amount of research on graph partitioning so that we refer the reader to overview papers [3–5, 27] for most of the general material. Here, we focus on parallel algorithms for high-quality graph partitioning.

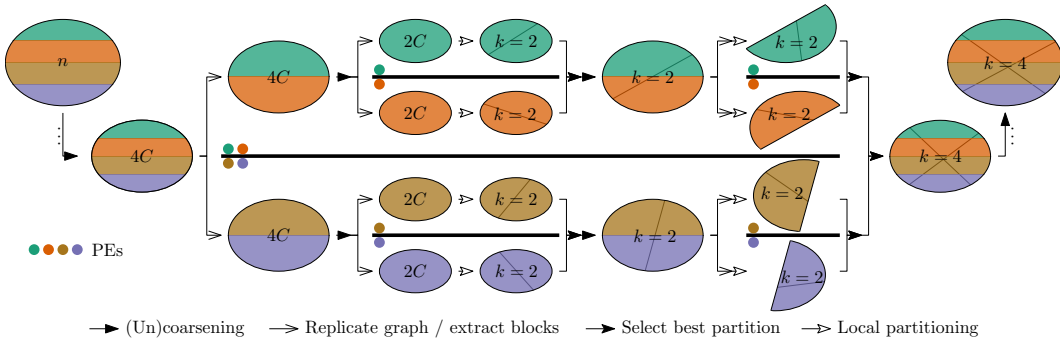
Distributed Graph Partitioning. Virtually all high-quality partitioners are based on the multilevel paradigm, e.g., ParMETIS [14, 15], ParHIP [23, 26] and others [6, 30]. These algorithms partition a graph in three phases. First, they build a hierarchy of successively coarse approximations of the input graph, usually by contracting matchings or clusters. Once the graph has only few vertices left (e.g., $n \leq Ck$ for some *contraction limit* C), the graph is partitioned into k blocks. Finally, this partition is successively projected onto finer levels of the hierarchy and refined using local search algorithms.

The performance of multilevel algorithms is defined by the algorithmic components used for these phases. Partitioners designed for mesh-partitioning usually contract matchings to coarsen the graph [6, 15, 30]. However, this technique is not suitable for partitioning complex networks that only admit a small maximum matching. Thus, other partitioners use two-hop matchings [17] or size-constrained label propagation [11, 13, 23]. Due to its simple yet effective nature, the latter is also commonly used as a local search algorithm during refinement [2, 8, 11, 13, 15, 23, 30].

Label propagation has also been used by non-multilevel graph partitioning algorithms such as XtraPuLP [28], which reports scalability up to 2^{17} cores, a level which has not been reached by multilevel algorithms. However, using label propagation without the multilevel paradigm comes with a pronounced decline in quality; Ref. [11] reports edge cuts for PuLP [29] (non-multilevel) that are on average more than twice as large and those of KaMinPar (multilevel). Across a large and diverse benchmark set, this is considered a lot; most multilevel algorithms achieve average edge cuts within a few percentage points of each other.

Another class of highly scalable graph partitioners include geometric partitioners, which work on a geometric embedding of the graph. While these algorithms are orders of magnitude faster than multilevel algorithms [19], they generally compute larger edge cuts and only work on graphs with a meaningful geometric embedding.

Deep Multilevel Graph Partitioning. As plain MGP algorithms usually shrink the graph down to Ck vertices, large values for k break the assumption that the coarsest graph is small. This causes their performance to deteriorate [11]. Instead, recursive bipartitioning can be used to compute partitions with large k , but this induces an additional $\log k$ factor



■ **Figure 1** Distributed deep multilevel graph partitioning on $P = 4$ PEs. Unpartitioned graphs are labeled with their number of vertices, partitioned graphs are labeled with their number of blocks. Blocks are subdivided into $K = 2$ blocks, and the goal is to partition to graph into $k = 4$ blocks.

in running time and makes it more difficult to compute balanced partitions due to the lack of global view. *Deep multilevel graph partitioning* (deep MGP) [11] circumvents these problems by continuing coarsening deep into initial partitioning. More precisely, deep MGP coarsens the graph until only $2C$ vertices are left, independent of k . Hereby, parallelism is exploited by maintaining the invariant that each PE processes at least C vertices, which is ensured by replicating coarser graphs and splitting the available PEs whenever the invariant would be violated. After bipartitioning the coarsest graphs, it maintains the invariant that a (coarse) graph with n vertices is partitioned into $\min\{k, n/C\}$ blocks by using recursive bipartitioning on the current level. By using additional balancing techniques, partitioners based on deep MGP can obtain feasible high-quality partitions with a large number of blocks (e.g., $k \approx 1M$) while often being an order of magnitude faster than partitioners based on plain MGP. Compared to recursive bipartitioning the entire graph, it reduces the additional $\log k$ factor to $\log kC/n$. KaMinPar [11] is a scalable shared-memory implementation of deep MGP which uses size-constrained label propagation during coarsening and refinement.

4 Distributed Deep Multilevel Graph Partitioning

We introduce dKaMinPar, a distributed graph partitioner based on deep MGP. We first describe the distributed deep MGP scheme itself, simplified by assuming that k and P are powers of two. Then, we outline the building blocks for coarsening, initial partitioning, refinement and balancing implemented in dKaMinPar.

Distributed Deep Multilevel Graph Partitioning. We outline the partitioning scheme in Figure 1 and Algorithm 1. Distributed deep MGP starts by coarsening the input graph down to $K \cdot C$ vertices, building a hierarchy of successively coarse graphs G_1, \dots, G_ℓ (Figure 1, left, and Algorithm 1, lines 6–8). Here, C is the *contraction limit* and K is a tuning parameter that generalizes the bipartitioning steps from Ref. [11] to K -way partitioning. To improve scalability on coarse levels, we follow Ref. [30] and maintain the invariant that P PEs work on a graph with at least $P \cdot C$ vertices by splitting the PEs into groups and duplicating the current graph whenever this invariant would be violated otherwise (lines 2–5). Once coarsening converged, we gather the coarsest graph G_ℓ on all PEs and partition it into $\min\{k, K\}$ blocks using a non-distributed graph partitioner (Figure 1, middle). The best partition (within each group of PEs) is selected and projected onto $G_{\ell-1}$. From here, we maintain two invariants: (1) the current partition is feasible, which is ensured by using

■ **Algorithm 1** DeepMGP(G, k, P): Deep multilevel with k blocks on P PEs.

```

Input:  $G = (V, E)$ ,  $k$ , const.  $C, K$ 
Output:  $k$ -way partition  $\Pi$  of  $G$ 
1 if  $|V(G)| > C \cdot \min\{k, K\}$  then // deep coarsening
2   if  $|V(G)| < C \cdot P$  then // duplicate graph if too small for  $P$  PEs
3      $c := P / \text{ceil}_2(|V(G)|/C)$  // number of copies
4      $G := \text{Replicate}(G, c)$  // replicate graph  $c$  times and group PEs
5      $P := P/c$  // number of PEs per group
   // standard multilevel graph partitioning:
6    $G_c := \text{Coarsen}(G)$ 
7    $\Pi_c := \text{DeepMGP}(G_c, k, P)$ 
8    $\Pi := \text{Project}(G, \Pi_c)$ 
9    $\Pi := \text{BalanceAndRefine}(G, \Pi)$ 
10 else // base case
11    $\Pi := \{V\}$  // trivial 1-way partition
12  $k' := \min\{k, \text{ceil}_2(|V|/C)\}$ 
13 while  $|\Pi| < k'$  do // extend partition
14    $G'_1, \dots, G'_{|\Pi|/P} := \text{DistributeBlocks}(G, \Pi)$  //  $G'_i$ s are local graphs
   // partition each local graph into  $\min\{k'/|\Pi|, K\}$  blocks:
15   for  $i := 1$  to  $|\Pi|/P$  do
16      $\Pi'_i := \text{LocalPartitioning}(G'_i, \min\{k'/|\Pi|, K\})$ 
   // combine local partitions  $\Pi'_i$  of  $G'_i$  to global partition  $\Pi$  of  $G$ :
17    $\Pi := \text{CollectPartitions}(\Pi'_1, \dots, \Pi'_{|\Pi|/P})$ 
18    $\Pi := \text{BalanceAndRefine}(G, \Pi)$ 
19 return  $\Pi$ 

```

the distributed balancing algorithm described below, and (2) a graph with n_ℓ vertices is partitioned into $\min\{k, \text{ceil}_2(n_\ell/C)\}$ blocks. Here, $\text{ceil}_2(x)$ denotes the smallest power of 2 equal to or larger than x . The second invariant is maintained using recursive K -way partitioning. More precisely, whenever the invariant is violated, we extract the block-induced subgraphs of the current partition and gather them on PEs such that each PE receives k/P complete subgraphs (note that $k \geq P$ due to the duplication process described above). From there, we use a non-distributed graph partitioner to recursively partition the subgraphs and project the new partitions back onto the distributed graph. This process is illustrated by Algorithm 1, lines 13–18. The resulting partition, satisfying both invariants, is then improved using a distributed k -way refinement algorithm. Note that if $k > \text{ceil}_2(|V(G_1)|/C)$, the partition computed on the finest graph has not enough blocks. In this case, we distribute and partition the block-induced subgraphs once more to compute the missing blocks (omitted from Algorithm 1).

Coarsening. We use a similar parallelization of size-constrained label propagation as ParHIP [23] and KaMinPar [11]. The algorithm works by first assigning each vertex to its own cluster. In further iterations over the vertices (we use $\{3, 5\}$ iterations), they are then moved to adjacent clusters such that the weight of intra-cluster edges is maximized without violating the maximum cluster weight $W := \varepsilon \frac{c(V)}{k'}$ where $k' := \min\{k, |V|/C\}$ [11].

6 Distributed Deep Multilevel Graph Partitioning

As noted in Ref. [2, 22], the solution quality of label propagation is improved when iterating over vertices in increased degree order. Since this is not cache efficient and lacks diversification by randomization, we sort the vertices into exponentially spaced degree buckets, i.e., bucket i contains all vertices with degree $2^i \leq d < 2^{i+1}$, and rearrange the input graph accordingly. This happens locally on each PE, i.e., we do not sort the vertices globally. Then, during label propagation, we split buckets into small chunks and randomize traversal on an inter-chunk and intra-chunk level. This is analogous to the randomization of the matching algorithm used by Metis [14].

To communicate the current cluster assignment of interface vertices, we follow ParHIP and split each iteration into $\max\{\alpha, \beta/P\}$ (we use $\alpha = 8$, $\beta = 128$) batches. After each batch, we use a sparse all-to-all operation to notify adjacent PEs of interface vertices that were moved to a different cluster. Since clusters can span multiple PEs, enforcing the maximum cluster weight becomes more challenging than in a shared-memory setting. ParHIP relaxes the weight limit and only enforces it locally, i.e., allows clusters with weight up to $P \cdot W$. This can lead to very heavy coarse vertices, making it more difficult to compute balanced partitions. Instead, we track the global cluster weights by sending the change in cluster weight after each batch to the PE owning the initial vertex of the cluster, which accumulates the changes and replies with the total weight of the cluster. If a cluster becomes heavier than W , each PE reverts moves proportional to its part of the total cluster weight. Those vertices can then be moved to other clusters during the next iteration.

After clustering the graph, we contract all clusters to build the next graph in the hierarchy. We give more details on this operation in Section 5.

Refinement. We also use size-constrained label propagation to improve the current graph partition. In contrast to label propagation for clustering as described above, vertices are initially assigned to clusters representing the blocks of the partition, and the maximum block weight is used as weight constraint. We use the same iteration order and number of batches as during coarsening to move vertices to adjacent blocks such that the weight of intra-block edges is maximized without violating the balance constraint. Ties are broken in favor of the lighter block, or by coin flip if both blocks have the same weight.

Since the number of blocks during refinement is usually much smaller than the number of clusters during coarsening, we track the global block weights using an allreduce operation after each vertex batch. Note that this does not prevent violations of the balance constraint if multiple PEs move vertices to the same block during the same vertex batch. In this case, we use our global balancing algorithm described below afterwards to restore the balance constraint. This is a downside compared to refinement via size-constrained label propagation in shared-memory parallel graph partitioners, where the balance constraint can be strictly enforced using atomic compare-and-swap operations.

Balancing. As noted in Ref. [11], balance constraint violations during deep MGP can occur after initial partitioning or after projecting a coarse graph partition onto a finer level of the graph hierarchy. Since these balance constraint violations are bounded by the weight of the heaviest vertex, we design the following balancing algorithm following the assumption that only few vertex moves are necessary to restore balance and that thus, it is feasible to invest a moderate amount of work per vertex movement. The greedy algorithm works as follows.

For each overloaded block B , we maintain a priority queue P_B of local vertices of that block on each PE. The vertices in the priority queues are ordered by their *relative gain*, which we define as $g \cdot c(v)$ if $g \geq 0$ and $g/c(v)$ if $g < 0$, where g is the largest reduction in edge cut

when moving v to a block that would not become overloaded. Note that this rating function generally prefers to move few heavy vertices over moving many lighter vertices, which follows our assumption that few vertex moves are sufficient to balance the partition. To keep the priority queues small, we maintain the invariant that a priority queue P_B stores no more vertices than are necessary to remove all excess weight $o(B) := c(B) - L_{\max}$ from B . We initialize the priority queues by iterating over the vertices. If a vertex is in an overloaded block B and $c(P_B) < o(B)$, we insert it. Otherwise, we only insert the vertex if its relative gain is larger than the lowest relative gain of any vertex in P_B and remove its lowest vertex if $c(P_B) > o(B) + \max_v c(v)$ after insertion.

After initializing the priority queues, we use a binary tree reduction to repeatedly identify the ℓ highest scored vertices per block globally, for some constant input parameter ℓ . For each overloaded block, each PE contributes up to ℓ vertices from its local priority queue. At each level of the reduction tree, the two lists of size $\leq \ell$ are then merged and cut off after at most ℓ vertices, or sooner if a shorter prefix is sufficient to remove all excess weight from the corresponding block. The root PE then decides which moves to perform such that no block becomes overloaded and broadcasts its decision to all PEs. Using this information, PEs remove vertices that were moved from their priority queues and update the relative gain of neighbors of moved vertices. We repeat this process until the partition is balanced.

5 Implementation Details

Vertex and Edge IDs. To reduce the communication overheads, we distinguish between local- and global vertex- and edge identifiers. This allows us to use 64 bit data types for global and 32 bit data types for local IDs.

Graph Contraction. Contracting a clustering consisting of n_C clusters and constructing the corresponding coarse graph works as follows. First, the clustering algorithm described above assigns a cluster ID to each vertex, which corresponds to some vertex ID in the distributed graph. We say that a cluster is *owned* by the PE owning the corresponding vertex. After contracting the local subgraphs (i.e., deduplicating edges between clusters and accumulating vertex- and edge weights), we map clusters to PEs such that each PE gets roughly the same number of coarse vertices while attempting to minimize the required communication amount. We assign $\leq \delta \cdot n_C / P$ clusters owned by each PE to the same PE (in our experiments, $\delta = 1.1$). If a PE owns more clusters, we redistribute the remaining clusters to PEs that have the smallest number of clusters assigned to them. Afterwards, each PE sends outgoing edges of coarse vertices to the respective PE using an all-to-all operation, then builds the coarse graph by deduplicating edges and accumulating vertex- and edge weights.

Low-latency Sparse All-to-All. Many steps of dKaMinPar require communication along the cut edges of the distributed graph, which translates to (often very) sparse and irregular all-to-all communication. Since `MPI_Alltoallv` has relatively high latency, we instead use a two-level approach that arranges PEs in a grid [25]. Then, messages are first sent to the right row, then to the right column, reducing the total number of messages sent through the network from $\mathcal{O}(P^2)$ to $\mathcal{O}(P)$.

6 Experiments

We implemented the proposed algorithm `dKaMinPar` in C++ and compiled it using `g++-12.1` with flags `-O3 -march=native`. We use OpenMPI 4.0 as parallelization library and `growt` [21] for hash tables. The raw data of all experiments is available online².

Setup. We evaluate the solution quality of our algorithm on a shared-memory machine equipped with 1 TB of main memory and one AMD EPYC 7702P processor with 64 cores (Machine A). Additionally, we perform scalability experiments on a high-performance cluster where each compute node is equipped with 256 GB of main memory and two Intel Xeon Platinum 8368 processors (Machine B). The compute nodes are connected by an InfiniBand 4X HDR 200 GBit/s network with approx. 1 μ s latency. We only use 64 out of the available 78 cores since some of the graph generators require the number of cores to be a power of two. While our partitioner can use multiple threads per MPI process, we only evaluate the configuration with one thread per MPI process, since this usually gives the best performance.

We compare `dKaMinPar` against the distributed versions of the algorithms included in Ref. [11], i.e., `ParHIP` [23] (v3.14) and `ParMETIS` [15] (v4.0.3). We do not include the distributed version `PuLP` [29] (`XtraPuLP` [28]) in our main comparison, since its quality is not competitive with multilevel partitioners. Instead, a comparison against `XtraPuLP` is available in Section 12. We evaluate two configurations of our algorithm: `dKaMinPar-Fast` uses $C = 2000$ as contraction limit (same as in Ref. [11]), `KaMinPar` [11] for initial partitioning and performs 3 iterations of label propagation during coarsening, whereas `dKaMinPar-Strong` uses $C = 5000$ (same as in Ref. [23]), `Mt-KaHyPar` [13] for initial partitioning and 5 iterations of label propagation during coarsening.

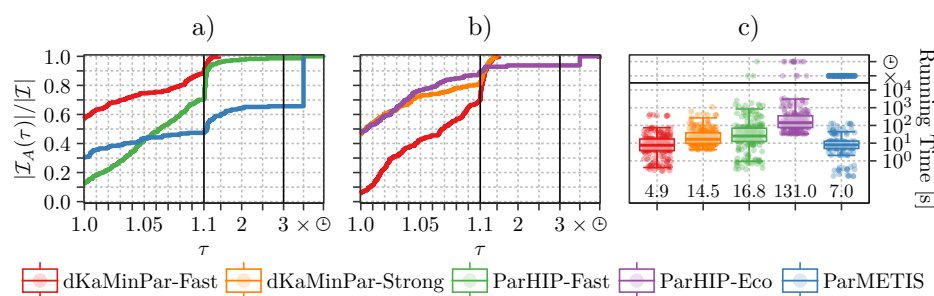
Instances. We evaluate our algorithm on the graphs from benchmark set B of Ref. [11] and the graphs used in Ref. [23]. A list of all graphs is available in Table 1, Section 8. Additionally, we use the graph generator `KaGen` [10] to evaluate the scaling capabilities of our algorithm on huge randomly generated 2D and 3D geometric and hyperbolic graphs denoted `rgg2DNdD`, `rgg3DNdD` and `rhg3,0NdD`. These graphs have 2^N vertices per compute node (64 cores) and average degree D . The random hyperbolic graphs have power-law exponent 3. The largest graphs of these families have 2^{33} vertices and 2^{39} edges.

Methodology. We call a combination of a graph and the number of blocks an *instance*. For each instance, we perform 5 repetitions with different seeds and aggregate the edge cuts and running times using the arithmetic mean. To aggregate over multiple instances, we use the geometric mean.

To compare the solution quality of different algorithms, we use *performance profiles* [9]. Let \mathcal{A} be the set of algorithms we want to compare, \mathcal{I} the set of instances, and $q_A(I)$ the quality of algorithm $A \in \mathcal{A}$ on instance $I \in \mathcal{I}$. For each algorithm A , we plot the fraction of instances $\frac{|\mathcal{I}_A(\tau)|}{|\mathcal{I}|}$ (y -axis) where $\mathcal{I}_A(\tau) := \{I \in \mathcal{I} \mid q_A(I) \leq \tau \cdot \min_{A' \in \mathcal{A}} q_{A'}(I)\}$ and τ is on the x -axis. Achieving higher fractions at lower τ -values is considered better. For $\tau = 1$, the y -value indicates the percentage of instances for which an algorithm performs best.

Solution Quality and Running Time. We evaluate the quality and running time of `dKaMinPar` against competing distributed MGP algorithms using all 64 cores of Machine A. Here, we

² https://algo2.itl.kit.edu/seemaier/ddeep_mgp/



■ **Figure 2** Results for $k = \{2, 4, 8, 16, 32, 64, 128\}$ with $\varepsilon = 3\%$ on Machine A. From left to right: (a) edge cuts of dKaMinPar-Fast, ParHIP-Fast and ParMETIS, (b) edge cuts of dKaMinPar-Fast, dKaMinPar-Strong and ParHIP-Eco, (c) running times of all algorithms. The numbers above the x-axis are geometric mean running times [s] over all instances for which all algorithms produced a result. Timeouts are marked with \oplus , failed runs or infeasible results are marked with \times .

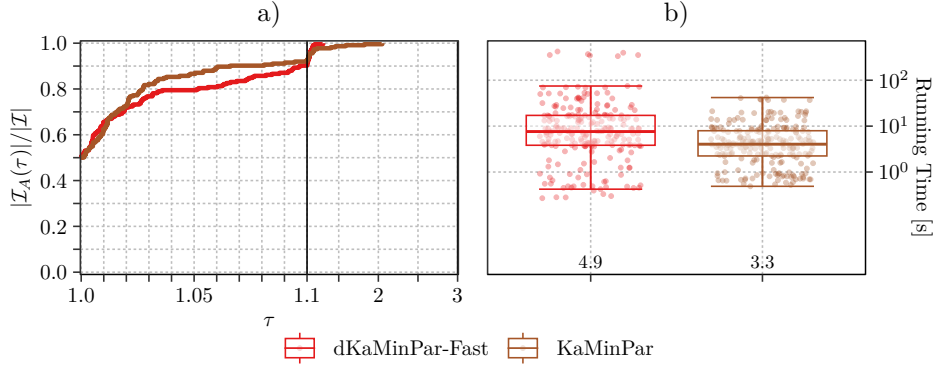
partition the graphs of our benchmark set into $k \in \{2, 4, 8, 16, 32, 64, 128\}$ blocks with $\varepsilon = 3\%$. To gain insights into the performance penalties of dKaMinPar due to its distributed nature, we also include a comparison against the shared-memory partitioner KaMinPar. Additionally, we report results for $k \in \{2^{11}, 2^{14}, 2^{17}, 2^{20}\}$ (*large k*) in Section 9. We set the time limit for a single instance to one hour, which is approx. 10 times the running time of dKaMinPar-Fast for small k on most instances³.

The results are summarized in Figure 2a–c. In Figure 2a, we can see that dKaMinPar-Fast finds the lowest edge cuts on approx. 60% of all benchmark instances, whereas ParMETIS and ParHIP-Fast only find better edge cuts on approx. 30% resp. 10% of all instances. Moreover, both competing algorithms frequently fail to compute feasible partitions — in particular, ParMETIS is unable to partition most social networks, violating the balance constraint or crashing on 34% of all instances. When looking at running times (Figure 2c), we therefore only average over those instances for which all partitioners computed a feasible partition or ran into the timeout (145 out of 224 instances). dKaMinPar-Fast (4.93s geometric mean running time) is 1.4 and 3.4 times faster than ParMETIS (6.98s) and ParHIP-Fast (16.77s), respectively. We attribute this to several reasons. Compared to ParMETIS, the lower running time is due to faster shrinkage of complex networks, while the advantage over ParHIP-Fast is due to our more cache-efficient implementation of label propagation, more efficient graph contraction and the low-latency sparse all-to-all implementation described in Section 5.

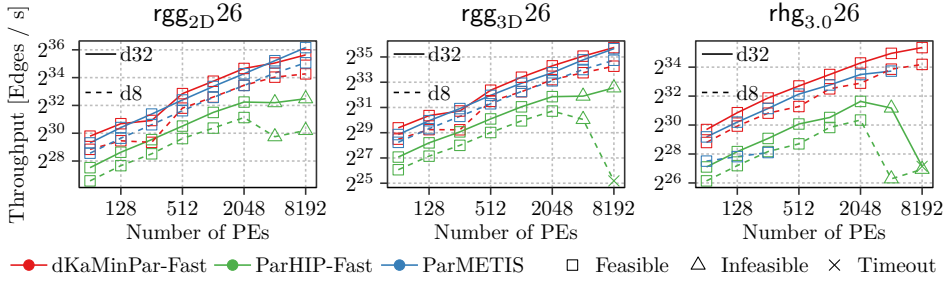
ParHIP also offers a strong configuration ParHIP-Eco, which performs more V-cycles and uses an evolutionary algorithm for initial partitioning to produce significantly better edge cuts at the cost of a much higher running time. In Figure 2b, we show that dKaMinPar can achieve the same solution quality when using the dKaMinPar-Strong configuration described above, while still being faster than ParHIP-Fast.

Finally, we compare our distributed partitioner against KaMinPar, which is a shared-memory implementation of deep multilevel graph partitioning with label propagation for coarsening and refinement. The results are summarized in Figure 3. The edge cut quality of both partitioners is almost the same, with a difference in average edge cut computed of less than 0.5%. However, the distributed partitioner is approx. 50% slower than the shared-memory partitioner. This is expected, as communication through message passing is generally less efficient than shared-memory communication.

³ Only twitter-2010 takes 6 min resp. 7 min for $k = 64$ resp. $k = 128$.



■ **Figure 3** Results for $k = \{2, 4, 8, 16, 32, 64, 128\}$ with $\varepsilon = 3\%$ on Machine A. From left to right: (a) edge cuts of dKaMinPar-Fast and KaMinPar, (b) corresponding running times. The numbers above the x-axis are geometric mean running times [s].

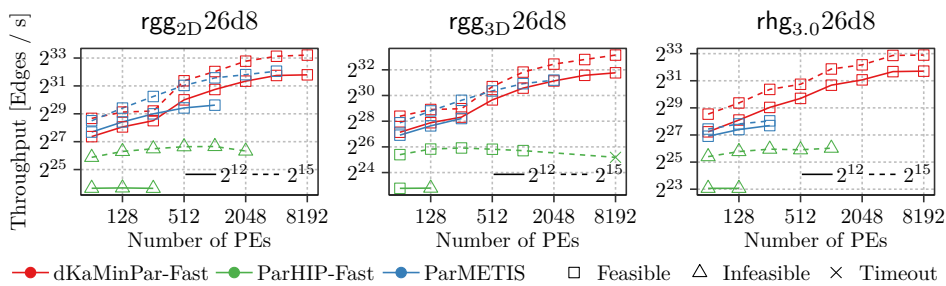


■ **Figure 4** Throughput of rgg_{2D} , rgg_{3D} and rhg graphs with 2^{26} vertices per compute node, average degree $\in \{8, 32\}$, $k = 16$ and $\varepsilon = 3\%$ on 64–8192 cores of Machine B.

Weak Scalability of dKaMinPar. We evaluate the weak scalability of dKaMinPar using 64–8192 cores (i.e., 1–128 compute nodes) of the high-performance cluster Machine B. For benchmark instances, we use randomly generated geometric (2D and 3D) and hyperbolic graphs with 2^{26} vertices per compute node and average degree $\in \{8, 32\}$.

In Figure 4, we partition these graphs into $k = 16$ blocks and observe weak scalability for dKaMinPar-Fast all the way to 8192 cores on all three graph families. On the geometric graphs, we achieve similar throughputs to ParMETIS, while ParHIP-Fast shows a drop in scalability beyond 2048 cores. This is most likely due to the extensive and inefficient communication performed by ParHIP-Fast during graph contraction. Moreover, we note that ParHIP-Fast was originally designed to overlap local work and global communication during label propagation through the use of nonblocking MPI operations. This implementation relies on MPI progression threads, which seem to be unavailable in modern OpenMPI versions. ParMETIS shows significantly worse throughputs on random hyperbolic graphs and is unable to compute a partition on 8192 cores. As mentioned before, this is most likely due to its inefficient coarsening strategy on graphs that follow a power-law degree distribution.

Looking at edge cuts (Table 3 in Section 10, upper half), ParMETIS finds lower edge cuts than dKaMinPar-Fast on the dense $rgg_{2D}26d32$ graph and both rgg_{3D} graphs by 5%–13%. However, on the sparser $rgg_{2D}26d8$ graph, dKaMinPar-Fast has 19% smaller cuts than ParMETIS which is already a considerable improvement. The gap gets much larger for the hyperbolic graph where ParMETIS only finds approx. 5.5–6.1 times larger cuts. Such solutions will be unsuitable for many applications.



■ **Figure 5** Throughput of rgg_{2D} , rgg_{3D} and rhg graphs with 2^{26} vertices per compute node, average degree 8, and $\varepsilon = 3\%$ on 64–8 192 cores of Machine B. The number of blocks are scaled with the size of the graph such that each block contains 2^{12} or 2^{15} vertices.

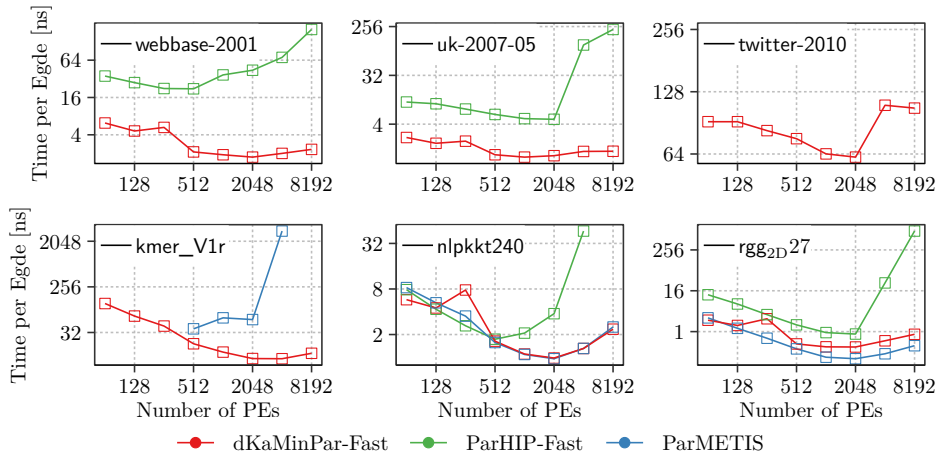
We now evaluate weak scalability in terms of graph size *and* number of blocks by scaling k with the number of compute nodes used. This implies that the number of blocks is large when using a large number of cores. The throughput of each algorithm in this setting is summarized in Figure 5. Note that we only use the sparser graphs in this experiment, since ParMETIS and ParHIP are unable to partition the dense versions of the graphs even on few compute nodes.

ParHIP-Fast is unable to obtain a feasible partition on all but 6 instances, none of which uses more than 1 024 cores, and only shows increasing throughputs up to 256 cores. While ParMETIS achieves decent weak scalability and computes feasible solutions on the mesh-type graphs, it is unable to partition any graph on 8 192 cores and often crashes on fewer cores (e.g., it only works on up to 1 024 cores on rgg_{2D} with 2^{12} vertices per block). On the random hyperbolic graph, it only computes a feasible solution on 64 cores. Meanwhile, dKaMinPar-Fast shows weak scalability up to 8 192 cores *on every graph family*, although it should be noted that the throughput increase from 4 096 to 8 192 is rather small.

In terms of number of edges cut, we summarize that dKaMinPar finds on average 19.3% and 2.8% lower edge cuts than ParMETIS and ParHIP-Fast, respectively (only averaging over instances for which the respective partitioner computed a feasible partition), with improvements ranging from 0% on $\text{rgg}_{3D}26d8$ to approx. 60% on $\text{rhg}_{3.0}d26$ (2^{15} vertices per block). Detailed per-instance edge cut results are available in Table 3 (Section 10).

Strong Scalability of dKaMinPar. We now look at strong scalability of dKaMinPar. Here, we partition three of the largest low- and high-degree graphs from our benchmark set into $k = 16$ blocks using 64–8 192 cores of Machine B and a time limit of 15 min. The results are summarized in Figure 6, where we can observe strong scalability for up to 1 024–2 048 cores on high-degree graphs. ParMETIS is unable to partition these graphs regardless of the number of cores used. While ParHIP-Fast scales up to 2 048 cores on uk-2007-05 , it should be noted that its running time is still higher than dKaMinPar on just 64 cores. The twitter graph is difficult to coarsen due to its highly skewed degree distribution; here, we observe that only dKaMinPar can partition the graph within the time limit.

Turning towards graphs with small maximum degree, we observe strong scalability for up to 2 048, 2 048 and 1 024 cores on kmer_V1r , nlpkt240 and $\text{rgg}_{2D}27$, respectively. Other algorithms seem to be unable to partition kmer_V1r , which ParMETIS is only able to partition on 512–4 096 cores, even though the graph is relatively small and fits into the memory of a single compute node. ParHIP-Fast is not able to partition the graph at all. Similar to our weak scaling experiments, ParMETIS shows better scalability and throughput on the



■ **Figure 6** Strong scaling running times for the largest low- and high-degree graphs in our benchmark set, with $k = 16$, $\varepsilon = 3\%$ on 64–8192 cores of Machine B.

mesh-type graph rgg_{2D} as well as on $nlpkkt240$.

The edge cuts obtained remain relatively constant (Table 4 in Section 11) when scaling to large number of cores. Surprisingly, the geometric mean edge cut on 8192 cores is slightly better than on 64 cores (by 2.0%).

7 Conclusion and Future Work

Our distributed-memory graph partitioner $dKaMinPar$ successfully partitions a wide range of input graphs using many thousands of cores yielding high speed and good quality. Further improvements of the implementation might be possible, for example making better use of shared-memory on each compute node. Beyond that, one can explore the quality versus time trade off. By distributed implementations of more powerful local improvement algorithms like local search or flow-based techniques one could achieve better quality at the price of higher execution time. It then also makes sense to look at a portfolio of different partitioners variants that can be run in parallel achieving good quality for subsets of inputs. For example, matching based coarsening as in $ParMETIS$ might help for mesh-like networks. On the other hand, more aggressive methods for handling high-degree nodes might help with some social networks.

References

- 1 Benchmarking for Graph Clustering and Partitioning. Encyclopedia of Social Network Analysis and Mining, Springer (2014)
- 2 Akhremtsev, Y., Sanders, P., Schulz, C.: High-Quality Shared-Memory Graph Partitioning. *IEEE Trans. Parallel Distributed Syst.* **31**(11), 2710–2722 (2020)
- 3 Bichot, C., Siarry, P. (eds.): Graph Partitioning. Wiley (2011)
- 4 Buluç, A., et al.: Recent Advances in Graph Partitioning. In: Algorithm Engineering — Selected Results and Surveys, LNCS, vol. 9220, pp. 117–158 (2016)
- 5 Çatalyürek, U.V., et al.: More Recent Advances in (Hyper)Graph Partitioning. *ACM Comput. Surv.* (2022)
- 6 Chevalier, C., Pellegrini, F.: PT-Scotch: A Tool for Efficient Parallel Graph Ordering. *Parallel Comput.* **34**(6–8), 318–331 (2008)

- 7 Davis, T.A., Hu, Y.: The University of Florida Sparse Matrix Collection. *ACM Trans. Math. Softw.* **38**(1), 1:1–1:25 (2011)
- 8 Devine, K.D., et al.: Parallel Hypergraph Partitioning for Scientific Computing. In: 20th International Parallel and Distributed Processing Symposium (IPDPS 2006)
- 9 Dolan, E.D., Moré, J.J.: Benchmarking Optimization Software with Performance Profiles. *Math. Program.* **91**(2), 201–213 (2002)
- 10 Funke, D., et al.: Communication-free Massively Distributed Graph Generation. *J. Parallel Distributed Comput.* **131**, 200–217 (2019)
- 11 Gottesbüren, L., et al.: Deep Multilevel Graph Partitioning. In: 29th European Symposium on Algorithms, (ESA) 2021. *LIPICs*, vol. 204, pp. 48:1–48:17. Schloss Dagstuhl - Leibniz-Zentrum für Informatik
- 12 Gottesbüren, L., Heuer, T., Sanders, P.: Parallel Flow-Based Hypergraph Partitioning. In: 20th International Symposium on Experimental Algorithms (SEA 2022). vol. 233, pp. 5:1–5:21. *LIPICs*
- 13 Gottesbüren, L., Heuer, T., Sanders, P., Schlag, S.: Scalable Shared-Memory Hypergraph Partitioning. In: 23rd Workshop on Algorithm Engineering and Experiments (ALENEX 2021). pp. 16–30. *SIAM*
- 14 Karypis, G., Kumar, V.: A Fast and High Quality Multilevel Scheme for Partitioning Irregular Graphs. *SIAM J. Sci. Comput.* **20**(1), 359–392 (1998)
- 15 Karypis, G., Kumar, V.: Multilevel k -way Partitioning Scheme for Irregular Graphs. *J. Parallel Distributed Comput.* **48**(1), 96–129 (1998)
- 16 LaSalle, D., Karypis, G.: Multi-threaded Graph Partitioning. In: 27th IEEE Int. Parallel and Distributed Processing Symposium (IPDPS). pp. 225–236 (2013)
- 17 LaSalle, D., et al.: Improving Graph Partitioning for Modern Graphs and Architectures. In: 5th Workshop on Irregular Applications - Architectures and Algorithms, (IA3) 2015. pp. 14:1–14:4. *ACM*
- 18 Leskovec, J., Krevl, A.: SNAP Datasets: Stanford Large Network Dataset Collection. <http://snap.stanford.edu/data> (2014)
- 19 von Looz, M., Tzovas, C., Meyerhenke, H.: Balanced k -means for Parallel Geometric Partitioning. In: 47th International Conference on Parallel Processing, (ICPP) 2018. pp. 52:1–52:10. *ACM*
- 20 o. M., U.: Laboratory of Web Algorithms. Datasets. <http://law.di.unimi.it/datasets.php>
- 21 Maier, T., Sanders, P., Dementiev, R.: Concurrent Hash Tables: Fast and General(?)! *ACM Trans. Parallel Comput.* **5**(4), 16:1–16:32 (2019)
- 22 Meyerhenke, H., Sanders, P., Schulz, C.: Partitioning Complex Networks via Size-Constrained Clustering. In: Experimental Algorithms - 13th International Symposium, (SEA) 2014. *LNCS*, vol. 8504, pp. 351–363. *Springer*
- 23 Meyerhenke, H., Sanders, P., Schulz, C.: Parallel Graph Partitioning for Complex Networks. *IEEE Trans. Parallel Distrib. Syst.* **28**(9), 2625–2638 (2017)
- 24 Raghavan, N., Albert, R., Kumara, S.: Near Linear Time Algorithm to Detect Community Structures in Large-Scale Networks. *Physical review. E, Statistical, nonlinear, and soft matter physics* **76**, 36–106 (2007)
- 25 Sanders, P., Schimek, M.: Engineering Massively Parallel MST Algorithms. In: 27th IEEE Int. Parallel and Distributed Processing Symposium (IPDPS) (2023)
- 26 Sanders, P., Schulz, C.: Think Locally, Act Globally: Highly Balanced Graph Partitioning. In: 12th Symposium on Experimental Algorithms, (SEA) 2013
- 27 Schulz, C., Strash, D.: Graph Partitioning: Formulations and Applications to Big Data. In: *Encyclopedia of Big Data Technologies*. *Springer* (2019)
- 28 Slota, G.M., et al.: Scalable, Multi-Constraint, Complex-Objective Graph Partitioning. *IEEE Trans. Parallel Distributed Syst.* **31**(12), 2789–2801 (2020)

14 Distributed Deep Multilevel Graph Partitioning

- 29 Slota, G.M., Madduri, K., Rajamanickam, S.: PuLP: Scalable Multi-Objective Multi-Constraint Partitioning for Small-World Networks. In: 2014 IEEE Int. Conference on Big Data (IEEE BigData 2014). pp. 481–490
- 30 Walshaw, C., Cross, M.: JOSTLE: Parallel Multilevel Graph-Partitioning Software — An Overview. Mesh Partitioning Techniques and Domain Decomposition Techniques pp. 27–58 (2007)

8 Benchmark Instances

■ **Table 1** Basic properties of the benchmark set. Graphs are roughly classified as *low degree* and *high degree* graphs based on their maximum degree Δ .

	Graph	n	m	Δ	Ref.
Low-degree graphs	packing	2 145 839	34 976 486	18	[1]
	channel	4 802 000	85 362 744	18	[1]
	hugebubbles	19 458 087	58 359 528	3	[1]
	nlpkkt240	27 993 600	746 478 752	27	[1]
	europa.osm	50 912 018	108 109 320	13	[1]
	kmerU1a	64 678 340	132 787 258	35	[7]
	rgg _{3D} 26	67 106 449	755 904 090	34	[10]
	rgg _{2D} 26	67 108 858	1 149 107 290	45	[10]
	del _{3D} 26	67 108 864	1 042 545 824	40	[10]
	del _{2D} 26	67 108 864	402 653 086	26	[10]
	rgg _{3D} 27	134 214 672	1 575 628 350	36	[10]
	rgg _{2D} 27	134 217 728	2 386 714 970	46	[10]
	del _{2D} 27	134 217 728	606 413 354	14	[10]
	del _{3D} 27	134 217 728	2 085 147 648	40	[10]
	kmerP1a	138 896 082	296 930 692	40	[7]
	kmerA2a	170 372 459	359 883 478	40	[7]
kmerV1r	214 004 392	465 409 664	8	[7]	
High-degree graphs	amazon	400 727	4 699 738	2 747	[18]
	eu-2005	862 664	32 276 936	68 963	[1]
	youtube	1 134 890	5 975 246	28 754	[18]
	in-2004	1 382 867	27 182 946	21 869	[1]
	com-orkut	3 072 441	234 370 166	33 313	[18]
	enwiki-2013	4 203 323	183 879 456	432 260	[20]
	enwiki-2018	5 608 705	234 488 590	248 444	[20]
	uk-2002	18 483 186	523 574 516	194 955	[1]
	arabic-2005	22 743 881	1 107 806 146	575 628	[20]
	uk-2005	39 454 463	1 566 054 250	1 776 858	[20]
	it-2004	41 290 648	2 054 949 894	1 326 744	[20]
	twitter-2010	41 652 230	2 405 026 092	2 997 487	[20]
	sk-2005	50 636 059	3 620 126 660	8 563 816	[20]
	uk-2007-05	105 153 952	6 603 753 128	975 419	[1]
	webbase-2001	115 554 441	1 709 619 522	816 127	[20]

9 Detailed Results for Large k

■ **Table 2** Edge cut and running time results for $k \in \{2^{10}, 2^{14}, 2^{17}, 2^{20}\}$ and $\varepsilon = 3\%$ on Machine A. The gmean imbalance of infeasible solutions is shown next to the number of infeasible solutions. The last two columns *rel. time* and *rel. cut* show the gmean running times and edge cuts relative to dKaMinPar-Fast of all instances for which the respective algorithm does not crash (timeout instances are additionally excluded in edge cut comparisons).

Algorithm	# timeout	# crash	# infeasible	# feasible	rel. time	rel. cut
dKaMinPar-Fast	0	0	0	128	1.00	1.00
ParHIP-Fast	6	48	57 (1.19)	17	22.21	1.06
ParHIP-Eco	39	40	37 (1.10)	12	88.35	0.96
ParMETIS	0	44	54 (1.18)	30	2.38	1.01
KaMinPar	0	0	0	128	0.46	0.98

As can be seen in Table 2, only partitioners based on (distributed) deep MGP consistently compute feasible partitions with a large number of blocks. ParHIP-Fast and ParMETIS only manage to do so on 17 and 30 out of 128 instances, respectively. We also note that ParHIP becomes quite slow, with even its fast configuration being more than an order of magnitude slower than dKaMinPar-Fast. This is because ParHIP keeps a relatively larger number of vertices per block in the coarsest graph ($C = 5000$), and is therefore unable to shrink the graph sufficiently even for moderate values of k .

10 Edge Cut Results for Weak Scaling

■ **Table 3** Edge cut results for weak scaling experiments on randomly generated graphs using 64–8 192 cores of Machine B and $\varepsilon = 3\%$. Some columns are not shown due to size constraints. Edge cuts and gmeans are reported relative to dKaMinPar-Fast. Timeouts (15 minutes) and crashes are marked with \ominus and \times , infeasible solutions are marked with \triangle .

Graph	Algorithm	Cut on number of PEs / 1000				gmean	
		128	512	2048	8192		
$k = 16$	rgg _{2D} 26d8	dKaMinPar-Fast	280	572	1177	2428	1.00
		ParHIP-Fast	1.10	1.13	1.14	\triangle	1.11
		ParMETIS	1.22	1.19	1.18	1.17	1.19
		XtraPuLP	87.12	131.52	333.21	637.60	190.28
	rgg _{2D} 26d32	dKaMinPar-Fast	4156	8544	17508	36050	1.00
		ParHIP-Fast	1.12	1.14	1.16	\triangle	1.15
		ParMETIS	0.95	0.94	0.94	0.94	0.94
		XtraPuLP	24.39	41.98	78.05	174.62	53.72
	rgg _{3D} 26d8	dKaMinPar-Fast	4668	12037	31526	81200	1.00
		ParHIP-Fast	1.01	1.01	1.00	\ominus	1.01
		ParMETIS	0.95	0.96	0.92	0.92	0.94
		XtraPuLP	12.48	19.92	25.31	37.47	21.13
	rgg _{3D} 26d32	dKaMinPar-Fast	40411	103491	267885	701865	1.00
		ParHIP-Fast	1.02	1.02	1.01	\triangle	1.02
		ParMETIS	0.88	0.87	0.86	0.84	0.87
		XtraPuLP	6.25	10.03	11.41	15.71	9.94
	rhg _{3.0} 26d8	dKaMinPar-Fast	3	11	6	3	1.00
		ParHIP-Fast	1.04	1.06	1.34	\triangle	1.20
		ParMETIS	4.85	\times	\times	\times	5.51
		XtraPuLP	9830.42	12480.89	77483.14	608259.52	48892.85
rhg _{3.0} 26d32	dKaMinPar-Fast	76	66	70	90	1.00	
	ParHIP-Fast	1.06	1.13	1.18	\ominus	1.12	
	ParMETIS	4.22	6.11	8.95	\times	6.07	
	XtraPuLP	1074.49	4613.94	17322.39	59519.97	6125.31	
2^{15} vertices per block	rgg _{2D} 26d8	dKaMinPar-Fast	5543	22517	90764	364279	1.00
		ParHIP-Fast	\triangle	\triangle	\triangle	\times	–
		ParMETIS	1.18	1.17	1.16	\times	1.17
		XtraPuLP	\triangle	\triangle	\times	\times	–
	rgg _{3D} 26d8	dKaMinPar-Fast	38348	156298	635175	2560517	1.00
		ParHIP-Fast	1.03	1.03	\times	\ominus	1.03
		ParMETIS	0.99	1.00	0.99	\times	1.00
		XtraPuLP	\triangle	\triangle	\times	\times	–
	rhg _{3.0} 26d8	dKaMinPar-Fast	1028	5157	19457	77084	1.00
		ParHIP-Fast	\triangle	\triangle	\times	\times	–
		ParMETIS	2.45	\times	\times	\times	2.52
		XtraPuLP	117.45	\times	\times	\times	115.92
2^{12} vertices per block	rgg _{2D} 26d8	dKaMinPar-Fast	16751	68202	277126	1109307	1.00
		ParHIP-Fast	\triangle	\times	\times	\times	–
		ParMETIS	1.09	1.07	\times	\times	1.08
		XtraPuLP	\times	\times	\times	\times	–
	rgg _{3D} 26d8	dKaMinPar-Fast	74560	300409	1213176	4876567	1.00
		ParHIP-Fast	\triangle	\times	\times	\times	1.03
		ParMETIS	1.00	\times	\times	\times	1.01
		XtraPuLP	\times	\times	\times	\times	–
	rhg _{3.0} 26d8	dKaMinPar-Fast	7255	30901	123132	495273	1.00
		ParHIP-Fast	\triangle	\times	\times	\times	–
		ParMETIS	1.67	\times	\times	\times	1.67
		XtraPuLP	\times	\times	\times	\times	–

11 Edge Cut Results for Strong Scaling

■ **Table 4** Edge cut results for strong scaling experiments on 64–8 192 cores of Machine B, $k = 16$, $\varepsilon = 3\%$. Some columns are not shown due to size constraints. Edge cuts and gmeans are reported relative to dKaMinPar-Fast. Timeouts (15 minutes) and crashes are marked with \ominus and \times , infeasible solutions are marked with \triangle .

Graph	Algorithm	Cut on number of PEs / 1 000				gmean
		128	512	2 048	8 192	
High-degree graphs						
webbase-2001	dKaMinPar-Fast	9 634	9 618	9 602	9 524	1.00
	ParHIP-Fast	1.09	1.10	1.14	1.12	1.11
	ParMETIS	\times	\times	\times	\times	–
	XtraPuLP	2.62	3.30	6.13	13.79	5.20
uk-2007-05	dKaMinPar-Fast	4 093	4 138	4 176	4 064	1.00
	ParHIP-Fast	1.07	1.03	1.01	1.06	1.04
	ParMETIS	\times	\times	\times	\times	–
	XtraPuLP	42.94	116.57	185.19	264.43	125.13
twitter-2010	dKaMinPar-Fast	616 530	601 073	604 954	588 380	1.00
	ParHIP-Fast	\ominus	\ominus	\ominus	\ominus	–
	ParMETIS	\ominus	\times	\times	\times	–
	XtraPuLP	1.36	1.48	1.51	1.58	1.48
Low-degree graphs						
kmer_V1r	dKaMinPar-Fast	10 936	10 897	10 880	10 836	1.00
	ParHIP-Fast	\times	\times	\times	\times	–
	ParMETIS	\times	0.84	0.84	\ominus	0.84
	XtraPuLP	13.19	13.12	12.56	12.56	12.85
nlpkkt240	dKaMinPar-Fast	5 658	5 641	5 623	5 547	1.00
	ParHIP-Fast	0.99	1.00	1.00	\times	1.00
	ParMETIS	0.93	0.94	0.95	0.97	0.95
	XtraPuLP	3.44	3.88	2.80	2.43	3.09
rgg _{2D} ²⁷	dKaMinPar-Fast	349	349	350	347	1.00
	ParHIP-Fast	1.14	1.15	1.13	1.15	1.14
	ParMETIS	1.19	1.18	1.17	1.15	1.17
	XtraPuLP	72.87	150.46	259.72	194.77	153.46

12 Comparison against XtraPuLP

We compare dKaMinPar against the single-level partitioner XtraPuLP [28] (v0.3), which is a hybrid (OpenMPI+OpenMP) implementation of single-level label propagation. To avoid excessive running time overheads due to graph generation, we only execute XtraPuLP using a single thread per MPI process.

Strong scaling running times are shown in Figure 7, while weak scaling running times are shown in Figure 8 ($k = 16$) and Figure 9 ($\{2^{15}, 2^{18}\}$ vertices per block). The corresponding edge cuts are included in Table 4 (Section 11) and Table 3 (Section 10). Surprisingly, dKaMinPar shows higher throughputs on most tested real-world and artificial graphs, although it should be noted that the performance of XtraPuLP could likely be improved by running it with more threads per MPI process. Moreover, we note that the edge cuts computed are often significantly worse (by up to 5 orders of magnitude on $rhg_{8.3.0d26}$ partitioned on 8192 cores) than those of the multilevel partitioners.

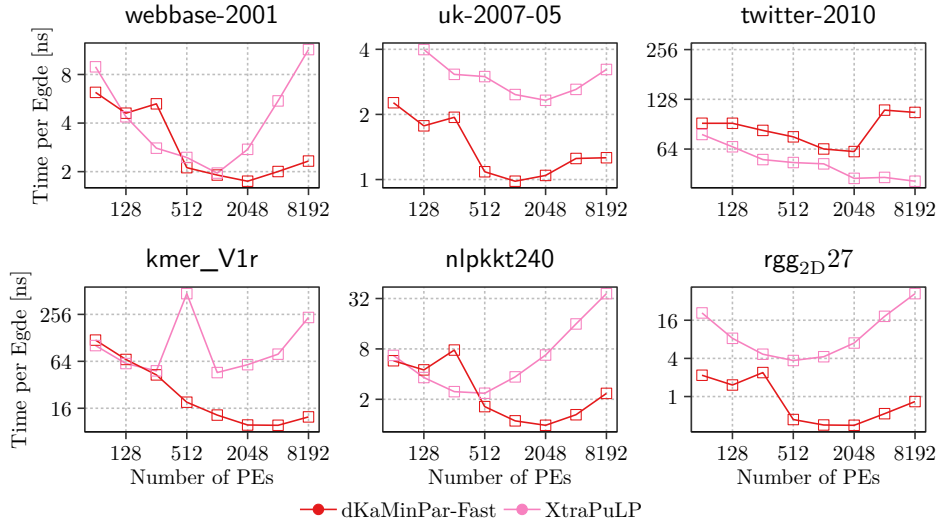


Figure 7 Strong scaling running times for the largest low- and high-degree graphs in our benchmark set, with $k = 16$, $\varepsilon = 3\%$ on 64–8192 cores of Machine B.

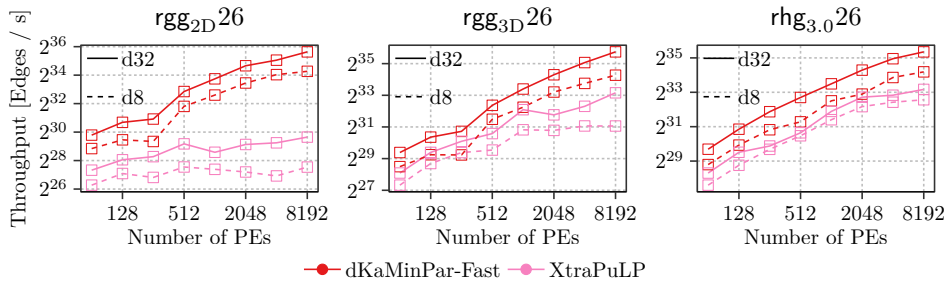
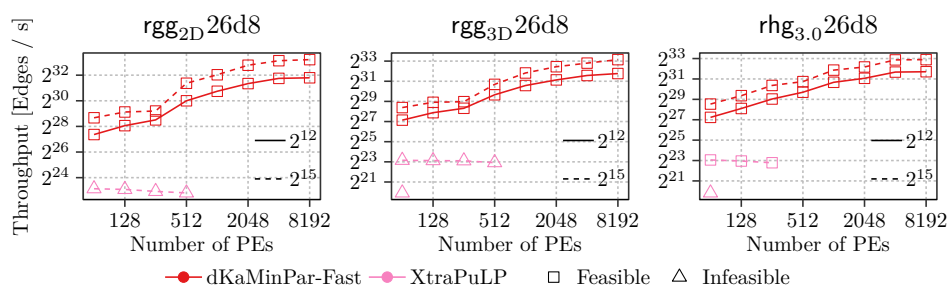


Figure 8 Throughput of rgg_{2D} , rgg_{3D} and rhg graphs with 2^{26} vertices per compute node, average degree $\in \{8, 32\}$, $k = 16$ and $\varepsilon = 3\%$ on 64–8192 cores of Machine B.



■ **Figure 9** Throughput of rgg_{2D} , rgg_{3D} and rhg graphs with 2^{26} vertices per compute node, average degree 8, and $\varepsilon = 3\%$ on 64–8192 cores of Machine B. The number of blocks are scaled with the size of the graph such that each block contains 2^{12} or 2^{15} vertices.